Mixed-Integer Linear Programming for Optimal Operation of the Integrated Electricity and Natural Gas System Considering Take or Pay Agreements

Ervina Nooraini [1)], Mohamad Almas Prakasa [2)], Muhammad Ruswandi Djalal [3)], Rony Seto Wibowo [4)], and Imam Robandi [5,*)]

[1, 2, 3, 4, 5)] Department of Electrical Engineering, Institut Teknologi Sepuluh Nopember, Surabaya, Indonesia

E-mail: ervinanaini@gmail.com[1)], 7022222015@student.its.ac.id[2)], 7022221006@student.its.ac.id[3)], ronyseto@yahoo.com[4)], and imam.robandi@its.ac.id[5)]

ABSTRACT

In the modern power system era, integrating electricity and natural gas systems increases the complexity of achieving optimal operation. Moreover, Take-or-Pay (TOP) agreements for natural gas lead to higher operating costs. Therefore, this paper is proposed to demonstrate the optimal operation of the Integrated Electricity and Natural Gas System (IENGS) by using Mixed-Integer Linear Programming (MILP) considering TOP agreements. The proposed methodology aims to optimize the total operating costs when TOP agreements are subjected to the IENGS while managing total power generation following the load demand. The proposed method is simulated on the integrated 6-bus electricity systems with 6-node natural gas systems. In this paper, the optimal operating cost is conducted in three scenarios. In the first scenario, optimal operation is conducted without TOP agreements, resulting in an optimal operating cost of $735,405.37. In the second scenario, the optimal operating costs range from $748,399.30 to $760,320.57 with the TOP agreement applied in one-by-one generators, which is 1.77% to 3.39% higher than without TOP agreements. In the third scenario, the optimal operating cost is $791,833.04 with the TOP agreement in all of the generators, which is 7.67% higher than without TOP agreements. The results have concluded that TOP agreements have increased the total operating cost by 1.77% to 7.67% in various TOP agreement scenarios. The MILP performance is validated by conducting the optimal operation in various TOP agreement scenarios without violating the power electricity balances, generator limits, transmission line capacities, and nodal gas flow balances.

Keywords: Integrated electricity and natural gas, mixed-integer linear programming, optimal gas flow, optimal power flow, take or pay agreement

Notations

C_{Gi} – Power generation cost of generator unit i ($/MW),
C_{mn} – Constant in the Weymouth equation of pipeline *m*-*n* (kcf/psig),
C_{Sm} – Gas production cost of gas source *m* ($/kcf),
EN_i – The number of electrical buses connected with bus *i*,
f – Vector of cost function,
F_{Ck} – Gas flow through compressor *k* (kcf),
F_{Dm} – Demand of gas node *m* (kcf),
F_{Gi} – Natural gas consumption in power plant-*i* (kcf),
F_{mn} – Gas flow from *m* to *n* pipelines (kcf),
F_{Sm} – Gas injection of source *m* (kcf),

* Corresponding author.
Received: March 17th, 2025. Revised: April 13th, 2025. Accepted: May 26th, 2025.
Available online: July 8th, 2025.

DOI: https://doi.org/10.12962/j24068535.v23i1.a1265

GC_m – Compressors with inlet node *m*,
GN_m – Gas nodes connected with node *m*,
GP_m – Gas-fired power plants with node *m*,
h – hour (unit of time),
i, j – Index of a bus, *i* = 1, 2, …, *N*,
k – Index of a compressor,
kcf – kilo cubic feet (unit of gas volume),
m, n – Index of a node, *m* = 1, 2, …, *M*,
max – Superscript indication of maximum value,
min – Superscript indication of minimum value,
P_{Gi}^t – Active power generation injected to bus *i* at time *t* (MW),
P_{ij}^t – Active power flow through line *i-j* at time *t* (MW),
P_{Li}^t – Electrical load demand of bus *i* at time *t* (MW),
psig – pounds per square inch gauge,
q^t – Gas supply for gas-fired power plant at time *t* (kcf),
q_{ToP} – Take-or-Pay contracted amount of gas supply (kcf),
rad – Radian (unit of angle),
t – Index of a time interval, *t* = 1, 2, …, *T*,
s – Index of gas flow equation segment, *s* =1, 2, …, *S*,
W – Watt (unit of power),
x_{ij} – Reactance of line *i-j* (ohm),
θ_i – Voltage angle of bus *i* (rad),
δ_i – Ramp rate of generation unit *i* (MW/h),
τ_k – Gas consumption of compressor *k* (kcf),
π_m – Gas pressure of node *m* (psig),
η_{Gi} – Coefficient of energy conversion in gas-fired power plant *i* (kcf/MW),
ϑ_k – Percentage of gas consumption in compressor *k*,
φ_{mn} – Squared gas pressure difference between node *m-n*,
μ_{mnS} – Segment *S* of gas flow equation through node *m-n*,

1. Introduction

Nowadays, the power and energy demand is relieved on coal-fired generators with fossil fuels [1]–[3]. With the projection of a global electricity increase of 2.1%/year, and it can triplet in 2050, the transition from traditional power generators to cleaner power generators should be considered [4]. The most popular effort is developing distributed power plants consisting of Renewable Energy Sources (RES), like solar photovoltaic units or wind generators [5]–[7]. It offers flexible implementation from small to large-scale power systems. However, the traditional power systems cannot be directly changed into RES. So the integration of natural-gas-fired generators with coal-fired generators becomes one of the viable options [8]. The use of natural gas-fired generators offers high efficiency, low capital cost, easy installation, and nearly zero emissions. For example, the average heat rate of natural gas-fired generators is 7,732 BTU/kWh, which is 27.43% lower than coal-fired generators [9]. In addition, it also has quick start-up and shut-down periods, which makes it a viable option for supporting base load and shaving peak load demand. Despite the many advantages, it requires long-term development to gradually replace the coal-fired

generators through the Integrated Electricity and Natural Gas System (IENGS) [10], [11], which can be supplied by Compressed Natural Gas (CNG) or Liquified Natural Gas (LNG) or mini-LNG, resulting a more economical, flexible, and cleaner power and energy production [12].

Besides the advantages, the optimal operation of IENGS becomes more challenging because more complex aspects should be considered [11]–[14]. For example, fluctuating pressure in the gas transmission pipelines can be caused by fluctuating gas consumption, which harms the safety and reliability of gas transmission. In addition, the interruption of the gas supply can cause power outages and load shedding that burden the gas-fired generators. Besides that, the coal and natural gas supplier company tends to implement the Take or Pay (TOP) agreements which must be adhered to by the power generation companies [15], [16]. The amount of coal and natural gas must be accurately calculated to avoid shortages or excess supply [17]. In [18], the TOP agreement has been investigated in the DOPF of a large power system. The result shows that the TOP agreement increases the total operating cost. Thus, this agreement becomes a crucial concern related to providing reliable and economical electricity for consumers and profits for the company. In the literature, the reports related to the optimal operation that considers the TOP agreement for natural gas are still limited.

In traditional power systems, the optimal operation can be obtained by the Dynamic Optimal Power Flow (DOPF) [19]. It is considered a viable option because it can represent the real operating conditions of the power systems by involving both technical and economic aspects, including ramp rate, voltage, transmission line capacity limitations, and others [6], [7]. The DOPF aims to calculate the minimum total generation cost in a specific period without violating any power system constraints. In the modern era, power system operation and control have been developed with robust programming methods [20], [21]. Mixed-Integer Linear Programming (MILP) is widely used for performing DOPF. For example, basic DC DOPF based on MILP is conducted in [22], [23]. Besides that, MILP formulation was conducted for AC OPF [24], [25]. In [26], MILP is used for DOPF for planning the expansion of the generation units and transmission systems. Based on [27], The use of MILP is balanced accuracy and complexity in power system optimization, including OPF. MILP has advantages in its reliability to conduct the optimum global solutions in a flexible and tractable way, especially in conducting optimal power flow for optimal operation of the power systems.

Along with the growth of IENGS, the DOPF is developed into Dynamic Optimal Power and Gas Flow (DOPGF) [28], [29]. Such as in [14], MILP is used to optimize natural gas and electricity transmission systems. The MILP implementation for DOPGF needs important modification, for example, the gas flow equation in IENGS should be linearized using the piecewise linear approximation [30], [31]. In [32]–[34], DOPGF with two MILP formulations has been developed utilizing the Special Order Sets (SOSs) feature and a two-stage piecewise linear mechanism. The result shows better accuracy and time in solving IENGS in large-scaled power systems than the basic MILP. From the mentioned literature, the optimal operation based on DOPGF using MILP for IENGS, considering the TOP agreement, has not yet been investigated. With a strong motivation to resolve the research gap, the contribution of this paper is the following.

1) This paper is proposed to demonstrate the optimal operation of the IENGS by using MILP considering TOP agreements. MILP based on DOPGF is demonstrated for optimizing the total operating costs when TOP agreements are subjected to the IENGS while managing total power generation following the load demand. The proposed method is simulated on integrated 6-bus electricity and 6-node natural gas systems.
2) An in-depth investigation of TOP agreements is conducted by simulating various scenarios: without TOP agreement, partial TOP agreement, and full TOP agreement. The MILP performance is validated by investigating the power electricity balances, generator limits, transmission line capacities, and nodal gas flow balances.

This paper is arranged as follows: In Section 2, the system modeling for power systems and problem definition are presented. In Section 3, the MILP implementation for DOPGF is demonstrated. In Section 4, the detailed results are discussed. In the rest, the main findings of this paper with the future recommendation are given in Section 5.

2. System Modeling and Problem Formulation

In this section, the IENGS model with detailed parameters is presented. The integration between the electricity system and the natural gas system is also explained. In addition, the problem definition is described.

2.1. IENGS Model

The IENGS constructed with the integration of 6-bus electricity and the 6-node natural gas systems are given in Fig. 1. Natural-gas-fired generators are supplied by natural gas systems through gas pipes. The electricity and the natural gas system is coupled by the natural gas-fired generator's output [35]. The electricity system has 4 power generators: Generator 1 (G1), Generator 2 (G2), Generator 3 (G3), and Generator 4 (G4). The constructed model has 3 electricity loads: Load 1 (L1), Load 2 (L2), and Load 3 (L3). The topology is in the following: G1 and G4 are located at Bus 1 and Bus 6 linked to Node 1 and Node 3 for the electricity and the natural gas system link. In addition, the natural gas system has 2 gas sources: Gas Source 1 (S1) and Gas Source 2 (S2), and 2 gas loads: Gas Load 1 (D1) and Gas Load 2 (D2). This model has also 5 branches consisting of 1 compressor and 4 pipelines.

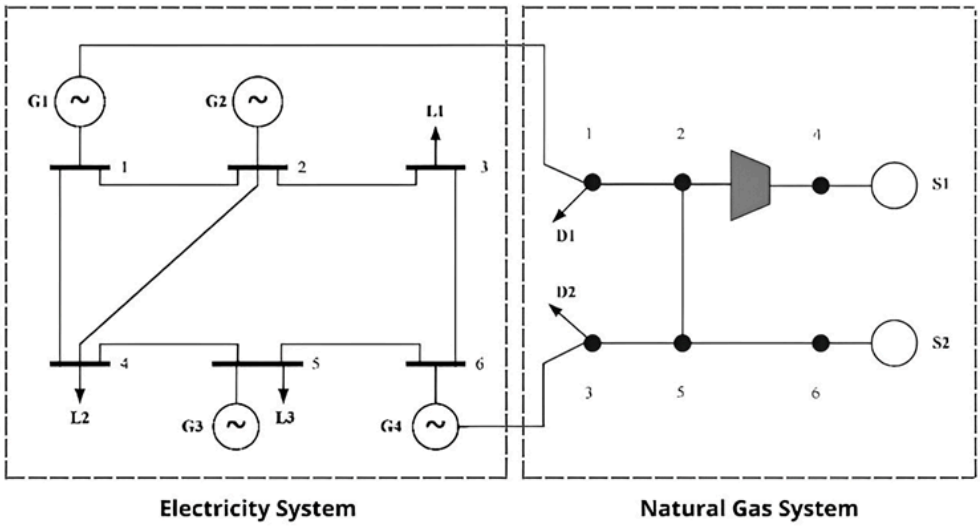

Fig. 1: IENGS model with 6-bus electricity and the 6-node natural gas systems

2.2. Objective Function

The DOPGF by suing MILP is formulated to calculate the optimal operating cost of IENGS. So, the formulated objective function, *f*(*obj*) is given in (1) with $C_{Gi}P_{Gi}^{t}$ is the fuel cost for natural gas-fired power generators and $C_{Sm}F_{Sm}^{t}$ is the cost of producing gas.

$$f(obj) = min\left[\sum_{t=1}^{T}\sum_{i=1}^{N} C_{Gi}P_{Gi}^{t} + \sum_{t=1}^{T}\sum_{m=1}^{M} C_{Sm}F_{Sm}^{t}\right] \quad (1)$$

2.3. Optimization Variables

In this paper, the optimization variables are the generation output of G1, G2, G3, and G4 as given in Table 1, and the natural gas output of S1 and S2, as given in Table 2. The typical parameters have been conducted from [34], [36]. Then, the optimization variables have been constrained by using electricity and natural gas limitations which are explained in the following sections.

Table 1: Parameters of coal-fired and gas-fired generators

Unit	Type	Cost Coefficient	P_{min} (MW)	P_{max} (MW)	Ramp (MW/h)
G1	Gas	0.147 kcf/ MW	30	100	15
G2	Coal	125 $/MW	30	100	5
G3	Coal	130 $/MW	30	100	5
G4	Gas	0.158 kcf/ MW	15	50	10

Table 2: Parameters of natural gas sources.

Unit	Node	Cost Coefficient	Minimum Output (kcf)	Maximum Output (kcf)
S1	5	2.5 $/kcf	1000	4500
S2	6	2 $/kcf	2000	6000

2.4. Electricity Constraints

The optimal power flow is performed by using Direct Current (DC) power flow with stable conditions of gas flow formulation adopted for modeling natural gas networks. In this paper, the in-flow and out-flow are assumed to be identical. First, the optimization has a DC power balance constraint as given (2), modified from [37].

$$P_{Gi}^{t} - P_{Li}^{t} = \sum_{j \in EN_i} \frac{\theta_i - \theta_j}{x_{ij}} \tag{2}$$

Second, the power system constraints are used as follows: the upper and lower generator limits as generation constraints as given in (3), the transmission line capacity constraints as given in (4), and the ramp rate of the generator is represented by (5).

$$P_{Gi}^{min} \leq P_{Gi}^{t} \leq P_{Gi}^{max} \tag{3}$$

$$-P_{ij}^{max} \leq P_{ij} \leq P_{ij}^{max} \tag{4}$$

$$-\delta_i \leq P_{Gi}^{t+1} - P_{Gi}^{t} \leq \delta_i \tag{5}$$

2.5. Natural Gas Constraints

A stable condition of gas flow can be formulated as (6) until (13). The nodal gas flow balance is given by (6).

$$F_{Sm} - F_{Dm} - \sum_{k \in GC_m} \tau_k - \sum_{i \in GP_m} F_{Gi} = \sum_{n \in GN_m} F_{mn} + \sum_{k \in GP_m} F_{Ck} \tag{6}$$

First, natural gas constraints are the upper and lower limits of gas production given by (7). The Weymouth gas flow equations are given by (8) and (9), modified from [31].

$$F_{Sm}^{min} \leq F_{Sm} \leq F_{Sm}^{max} \tag{7}$$

$$F_{mn} = sgn(\pi_m, \pi_n) C_{mn} \sqrt{|\pi_m^2| - \pi_n^2} \tag{8}$$

$$sgn(\pi_m, \pi_n) = \{1, \pi_m > \pi_n \; -1, \pi_m < \pi_n \tag{9}$$

Second, the gas consumption value of a natural gas-fired power generator and the generated power are used as constraints, given in (10). The gas consumption of the compressor is stated in (11).

$$F_{Gi} = \eta_{Gi} P_{Gi} \tag{10}$$

$$\tau_k = \vartheta_k F_{Ck} \tag{11}$$

In this paper, the gas of the compressor is formulated by a fixed percentage (ϑ_k) of the elated gas, and ϑ_k is assumed to be 3%. The pipeline gas flow limitation is represented by (12). The nodal gas pressure is given by (13).

$$0 \leq F_{mn} \leq F_{mn}^{max} \tag{12}$$

$$\pi_m^{min} \leq \pi_m \leq \pi_m^{max} \tag{13}$$

2.6. TOP Agreement Formulation as Constraint

In the optimization by using MILP, TOP agreements are used as constraints that ensure the gas fuel consumption is equal to the contracted amount (q_{ToP}), which are formulated as (14) and (15), modified from [17]. The gas

fuel consumption is adjusted to the power generation output using the gas-to-power conversion coefficient (η_G), subject to total fuel supply and contract period. TOP constraints are committed to daily and hourly constraints.

$$q^t = \eta_{Gi} P_{Gi}^t \tag{14}$$

$$\sum_{t=1}^{T} q^t = q_{ToP} \tag{15}$$

3. DOPGF based on MILP for IENGS

The flowchart of DOPGF using MILP which was performed for IENGS is shown in Fig. 2. The implementation step starts by modeling the IENGS as illustrated in Fig. 1, and defining the simulation parameters as given in Table 1 and Table 2. In the next step, the problem formulation is also conducted. In the following section, the MILP implementation for optimal operation of IENGS is explained.

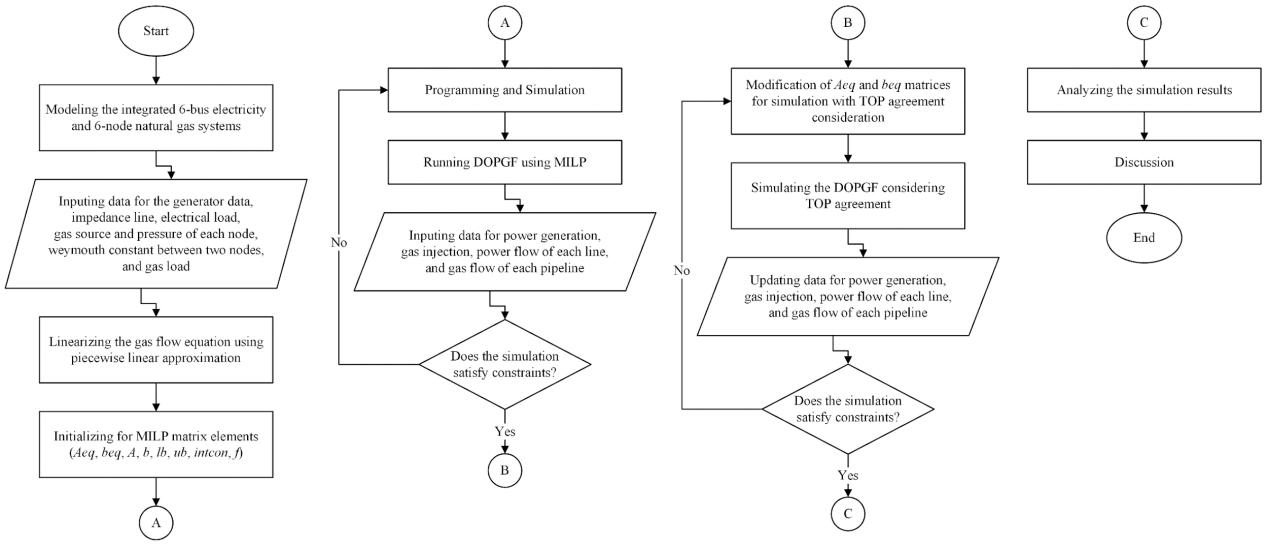

Fig. 2: Flowchart of DOPGF using MILP for IENGS.

3.1. Piece-wise Linear Approximation

Before the MILP implementation, the nonlinear and nonconvex gas flow equations should be linearized using piecewise linear approximation. The gas flow equation (F_{mn}) is linearized by φ_{mn}, so (16) can be replaced by (17) with φ_{mn} is calculated by (17).

$$F_{mn} = sgn(\pi_m, \pi_n) C_{mn} \tag{16}$$

$$\varphi_{mn} = \pi_m^2 - \pi_n^2 \tag{17}$$

The upper and lower bounds of nodal gas pressure are also linearized as (18) until (21).

$$\left(\pi_m^{min}\right)^2 \leq \pi_m^2 \leq \left(\pi_m^{max}\right)^2 \tag{18}$$

$$\left(\pi_n^{min}\right)^2 \leq \pi_n^2 \leq \left(\pi_n^{max}\right)^2 \tag{19}$$

$$\varphi_{mn}^{max} = \left(\pi_m^{max}\right)^2 - \left(\pi_n^{min}\right)^2 \tag{20}$$

$$\varphi_{mn}^{min} = \left(\pi_m^{min}\right)^2 - \left(\pi_n^{max}\right)^2 \tag{21}$$

with the φ_{mn} in the range $[\varphi_{mn}^{min}\ \varphi_{mn}^{max}]$ is calculated in the gas flow equation with the appropriate Weymouth constant value producing a nonlinear graph, then divided into several pieces using piecewise linear approximation

producing several linear graph segments and each piece of linear segment corresponds to an approximate value of the square function.

3.2. MILP Implementation

The DOPGF by using MILP for IENGS considering the TOP agreement should be defined in MILP forms. The objective function in MILP is represented by (22). The linear equality and inequality constraint are given by (23) and (24), respectively. The upper and lower bounds of each variable are represented by (25). In addition, the integer constraints are given by (26).

$$f(x) = min\ f^T x \tag{22}$$

$$A_{eq}.\ x = b_{eq} \tag{23}$$

$$A.x \leq b \tag{24}$$

$$lb \leq x \leq ub \tag{25}$$

$$x\ (intcon) \in \{..., -1, 0, 1, ...\} \tag{26}$$

In MILP, the optimization variables are provided in matrix form as shown in (27). The variables for the electricity network are the voltage angle of each bus (θ_N) and the power generation output of each generator (P_{GN}). While the optimization variables of the natural gas network are the squared gas pressure differences between two nodes (φ_{mnS}), natural gas injections (F_{SM}), and the selection of gas flow equation segments (μ_{mnS}).

$$x^T = [\theta_1 ... \theta_N\ P_{G1} ... P_{GN}\ \varphi_{211} ... \varphi_{mnS}\ F_{S1} ... F_{SM}\ \mu_{211} ... \mu_{mnS}] \tag{27}$$

Then, the selection of the natural gas flow segments is formulated by (28) with A_{eq} is arranged diagonally as t, while the vector b_{eq} is arranged vertically t.

$$\mu_{mn1} + \mu_{mn2} + ... + \mu_{mnS} = 1 \tag{28}$$

The inequality matrix of MILP of IENGS is represented by A and b which consist of transmission line capacity, generator ramp rate, and gas pipeline capacity which is linearized into (29) with matrix A is arranged diagonally as t, while the vector b is arranged vertically as t.

$$m_{mnS}.\ \varphi_{mnS} + b_{mnS}.\ \mu_{mnS} \leq F_{mn}^{max} \tag{29}$$

The lower and upper bound vectors are represented by lb and ub. The length of the column of matrix lb and ub is equal to the length of the column of optimization variables x as in (30) with lb and ub arranged vertically as much as t, and $intcon$ is arranged as t.

$$\begin{aligned} &[0 \ldots -inf\ \ P_{G1}^{min} \ldots P_{GN}^{min}\ \ \varphi_{12A}^{min} \ldots \varphi_{mnS}^{min}\ \ F_{S1}^{min} \ldots F_{SM}^{min}\ \ 0 \ldots 0\ \ ] \\ &\quad \leq [\theta_1 \ldots \theta_N\ \ P_{G1} \ldots P_{GN}\ \ \varphi_{121} \ldots \varphi_{mnS}\ \ F_{S1} \ldots F_{SM}\ \ \mu_{121} \ldots \mu_{mnS}\ \ ] \\ &\quad \leq [0 \ldots inf\ \ P_{G1}^{max} \ldots P_{GN}^{max}\ \ \varphi_{12A}^{max} \ldots \varphi_{mnS}^{max}\ \ F_{S1}^{max} \ldots F_{SM}^{max}\ \ 1 \ldots 1\ \ ] \end{aligned} \tag{30}$$

4. Simulation and Discussion

In this section, the simulation results for optimal operation of IENGS by using MILP considering TOP agreements are presented and discussed. The simulation is conducted on the MATLAB/Simulink environment that running on the device with the specifications described in the following: Processor Intel Core i5-7200U, ~2.5 GHz to~2.7 GHz, Nvidia GeForce 930MX 2 GB, 8 GB RAM DDR3, In this simulation, the 24-hour electrical load profile is used to simulate the operation behavior of IENGS as shown in Fig. 3. Before discussing the simulation results, the linearized natural gas flow which is determined based on the maximum and minimum pressure of the gas is shown in Table 3.

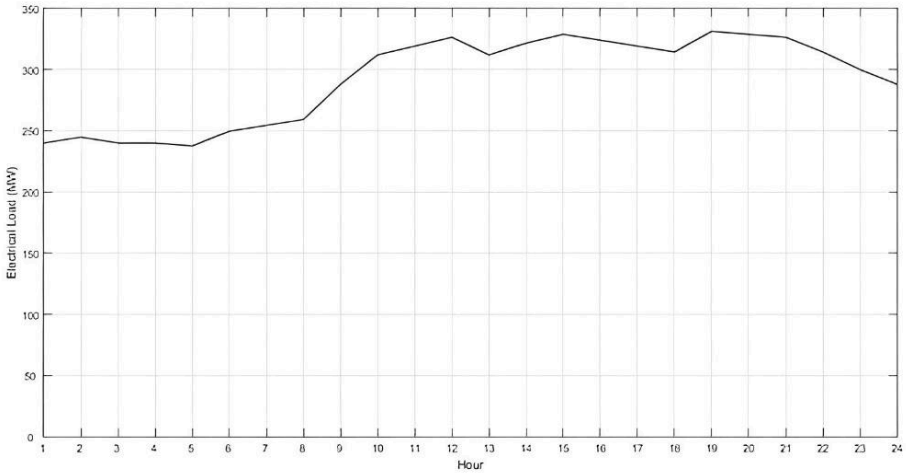

Fig. 3: The 24-hour electrical load profile for the IENGS simulation

Table 3: Gas pressure constraint for each node on the IENGS.

Node	π_{min} **(Psig)**	π_{max} **(Psig)**	π^2_{min} **(Psig^2)**	π^2_{max} **(Psig^2)**
1	105	120	11,025	14,400
2	120	135	14,400	18,225
3	125	140	15,625	19,600
4	130	155	16,900	24,025
5	140	155	19,600	24,025
6	150	175	22,500	30,625

In addition, φ_{mn} is determined with the appropriate constant value to produce a nonlinear graph and divided into several pieces to produce several linear graph segments as shown in Fig. 4. The final value for the natural gas flow equation is calculated by using Root Mean Square Error (RMSE) as tabulated in Table 4. Then, from Table 4, the average RMSE for the natural gas equation is 72,557.

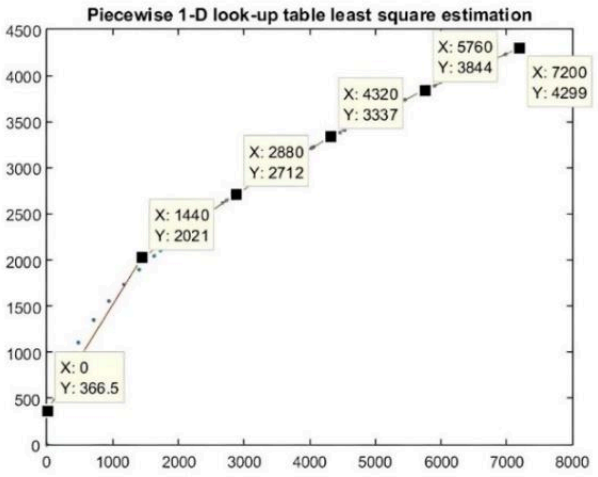

Fig. 4: Piecewise linear graph for natural gas flow equation.

The investigation regarding the optimal operation by using MILP considering TOP agreement is divided into three scenarios. The first scenario is conducted based on the IENGS without TOP agreements. Then, the optimal operating cost without a TOP agreement is identified as a base case. This base case will be used to justify the cost increase when TOP agreements are subjected to the IENGS. Furthermore, the amount of natural gas supply

Table 4: RMSE for natural gas flow equation.

No	From Node	To Node	RMSE
1	1	2	71,930
2	2	4	111,145
3	2	5	5,142
4	3	5	66,788
5	5	6	107,783
	Average		72,557

in the base case is investigated to determine the TOP agreements for the next scenarios, including partial and full implementation of TOP agreements.

4.1. Results for Scenario 1: Without TOP Agreements

The power generation of each generator and the gas consumption by gas-fired power generators in Scenario 1 are shown in Table 5 and Fig. 5, while the gas injection of each gas source is illustrated in Fig. 6. The generated power of units 1 to 4 suffice the maximum and minimum capacities of each unit. The total power generation fulfills the electrical load, which is 7,020 MW and the power generation of each hour satisfies the ramp rate of each generating unit. The gas injection of sources 1 and 2 suffice the minimum and maximum capacity of each source. The total gas injection fulfills the gas load, gas supply for natural-gas-fired power generators, and gas consumption of the compressor, with a total gas injection of 132,989.42 kcf, total gas fuel supply of 516.83 kcf, and gas consumption of the compressor of 847.59 kcf. Validation of the gas flow balance is carried out by ensuring the value of the gas that comes out is equal to the gas that enters each node. From the results, the out-flow gas at nodes 1 to 6 matches with the in-flow gas of each node, and the squared gas pressure variance between the two nodes satisfies the pressure limits of each segment. The optimal operating costs which consist of electricity generation and gas production costs are shown in Table 6. The natural gas production cost is $280,105.37, and the electricity production cost is $455,300.00. Thus, the total operating cost of the investigated IENGS by using MILP without the TOP agreement is $735,405.37. In the next discussion, this cost is used as the base case for calculating the cost increase due to TOP agreements.

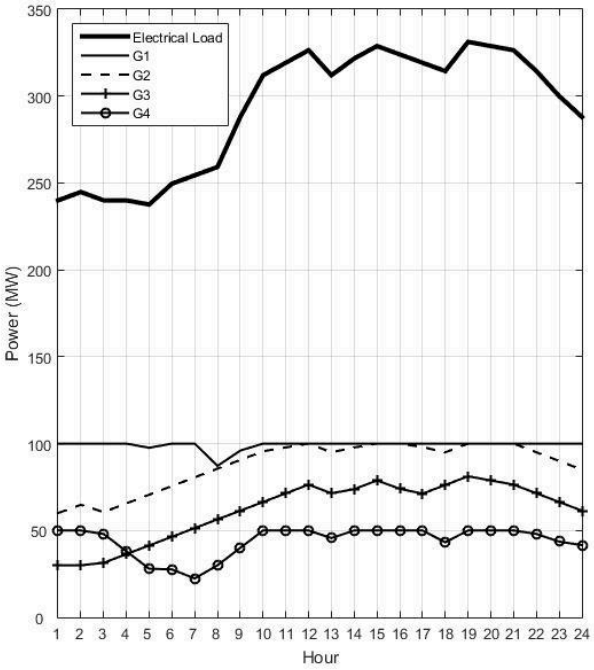

Fig. 5: Power generation for electrical load in Scenario I.

Table 5: Power generation and gas supply performances in Scenario I.

Hour	Power Generation (MW)				Gas Supply (kcf)	
	G1	G2	G3	G4	N1	N2
1	100	60	30	50	14.70	7.90
2	100	64.8	30	50	14.70	7.90
3	100	60.6	31.4	48	14.70	7.58
4	100	65.6	36.4	38	14.70	6.00
5	97.6	70.6	41.4	28	14.35	4.42
6	100	75.6	46.4	27.6	14.70	4.36
7	100	80.6	51.4	22.4	14.70	3.54
8	87.2	85.6	56.4	30	12.82	4.74
9	96	90.6	61.4	40	14.11	6.32
10	100	95.6	66.4	50	14.70	7.90
11	100	97.8	71.4	50	14.70	7.90
12	100	100	76.4	50	14.70	7.90
13	100	95	71.4	45.6	14.70	7.20
14	100	97.8	73.8	50	14.70	7.90
15	100	100	78.8	50	14.70	7.90
16	100	100	74	50	14.70	7.90
17	100	98	71.2	50	14.70	7.90
18	100	95	76.2	43.2	14.70	6.83
19	100	100	81.2	50	14.70	7.90
20	100	100	78.8	50	14.70	7.90
21	100	100	76.4	50	14.70	7.90
22	100	95	71.4	48	14.70	7.58
23	100	90	66.4	43.6	14.70	6.89
24	100	85	61.4	41.6	14.70	6.57
Total	**2380.8**	**2103.2**	**1480.0**	**1056.0**	**349.98**	**166.85**

Table 6: Optimal operating costs in Scenario I.

Gas Supply (kcf)		Gas Production Cost ($)	Generation Cost ($)	Total Operating Cost ($)
Node 1	Node 3			
349.98	166.85	280,105.37	455,300.00	735,405.37

4.2. Results for Scenario 2: Partial TOP Agreements

In Scenario 2, the IENGS is simulated with partial TOP agreements. The simulation is carried out by considering the TOP agreement one by one of the natural gas-fired power generators. In Scenario 2, the investigation is divided into 2 cases: the first case investigates the TOP implementation on G1 and the second case investigates the TOP implementation on G4. Based on the total natural gas supply in Scenario 1, the TOP agreement for natural gas for unit G1 is set to be 300 kcf/day while unit G4 is set to be 150 kcf/day. The power generation and natural gas supply performances in Scenario 2 are shown in Table 7 and Table 8. In Scenario 2, the implementation of the TOP agreement for natural gas has adjusted the total natural gas fuel with the contract value in units G1 and G4. For this scenario, the optimal operating costs in Scenario 2 are illustrated in Table 9 and Table 10. The implementation of the TOP agreement for natural gas in unit G1 increases the optimal operating cost by 3.39% of $760,320.57 from the base case. Meanwhile, the implementation of the TOP agreement for natural gas in unit G4 also increased the optimal operating cost by 1.77% of 748,399.30. This scenario concludes that the total operating cost increase for TOP implementation on G1 is higher than G4. These presented results have validated the MILP performance by conducting the optimal operation in various TOP agreement scenarios without violating the power electricity balances, generator limits, transmission line capacities, and nodal gas flow balances.

Table 7: Power generation and gas supply performances in Scenario 2 Case 1.

Hour	Power Generation (MW)				Gas Supply (kcf)	
	G1	G2	G3	G4	N1	N2
1	63	97	30	50	9.26	7.90
2	72.8	92	30	50	10.70	7.90
3	71.6	87	31.4	50	10.53	7.90
4	71.6	82	36.4	50	10.53	7.90
5	60.2	86	41.4	50	8.85	7.90
6	62.2	91	46.4	50	9.14	7.90
7	57	96	51.4	50	8.38	7.90
8	65.6	91	56.4	46.2	9.64	7.30
9	80.6	96	61.4	50	11.85	7.90
10	95.6	100	66.4	50	14.05	7.90
11	97.8	100	71.4	50	14.38	7.90
12	100	100	76.4	50	14.70	7.90
13	90.6	100	71.4	50	13.32	7.90
14	97.8	100	73.8	50	14.38	7.90
15	100	100	78.8	50	14.70	7.90
16	100	100	74	50	14.70	7.90
17	98	100	71.2	50	14.41	7.90
18	88.2	100	76.2	50	12.97	7.90
19	100	100	81.2	50	14.70	7.90
20	100	100	78.8	50	14.70	7.90
21	100	100	76.4	50	14.70	7.90
22	93	100	71.4	50	13.67	7.90
23	88.6	95	66.4	50	13.02	7.90
24	86.6	90	61.4	50	12.73	7.90
Total	**2,040.8**	**2,303.0**	**1,480.0**	**1,196.2**	**300.00**	**189.00**

Table 8: Power generation and gas supply performances in Scenario Case 2.

Hour	Power Generation (MW)				Gas Supply (kcf)	
	G1	G2	G3	G4	N1	N2
1	100	73,1	30	36,9	14,70	5,83
2	100	68,1	30	46,7	14,70	7,38
3	100	71,9	31,4	36,7	14,70	5,80
4	100	76,9	36,4	26,7	14,70	4,22
5	100	79,5	41,4	16,7	14,70	2,64
6	100	82,4	46,4	20,8	14,70	3,29
7	100	87,4	51,4	15,6	14,70	2,46
8	87,2	90	56,4	25,6	12,82	4,04
9	96	95	61,4	35,6	14,11	5,62
10	100	100	66,4	45,6	14,70	7,20
11	100	100	71,4	47,8	14,70	7,55
12	100	100	76,4	50	14,70	7,90
13	100	100	71,4	40,6	14,70	6,41
14	100	100	73,8	47,8	14,70	7,55
15	100	100	78,8	50	14,70	7,90
16	100	100	74	50	14,70	7,90
17	100	100	71,2	48	14,70	7,58
18	100	98,2	76,2	40	14,70	6,32
19	100	100	81,2	50	14,70	7,90
20	100	100	78,8	50	14,70	7,90
21	100	100	76,4	50	14,70	7,90
22	100	100	71,4	43	14,70	6,79
23	100	95	66,4	38,6	14,70	6,10
24	100	90	61,4	36,6	14,70	5,78
Total	**2.383,20**	**2.207,43**	**1.480,00**	**949,37**	**350,33**	**150,00**

Table 9: Operating costs in Scenario 2 Case 1.

Gas Supply (kcf)		Gas Production Cost ($)	Generation Cost ($)	Total Operating Cost ($)
Node 1	Node 3			
300	189	280,047.61	480,272.96	760,320.57

Table 10: Operating costs in Scenario 2 Case 2.

Gas Supply (kcf)		Gas Production Cost ($)	Generation Cost ($)	Total Operating Cost ($)
Node 1	Node 3			
350.33	150	280,070.19	468,329.11	748,399.30

4.3. Results for Scenario 3: Full TOP Agreements

In Scenario 3, the optimal operation of IENGS by using MILP is simulated by implementing the TOP agreements on all natural gas-fired generators, G1 and G4. The amount of natural gas supply for the TOP agreements in Scenario 3 is the same as in Scenario 2. In Scenario 3, the more comprehensive results and discussions are presented to show the IENGS operating behavior. First, the power generation comparisons of G1, G2, G3, and G4 from each scenario are illustrated in Fig. 6, Fig. 7, Fig. 8, and Fig. 9, respectively. Based on the results, natural-gas-fired power generators (G1 and G4) have a higher frequency of changes in generating power than coal-fired generators (G2 and G3), which indicates the flexibility of natural-gas-fired power generator operations.

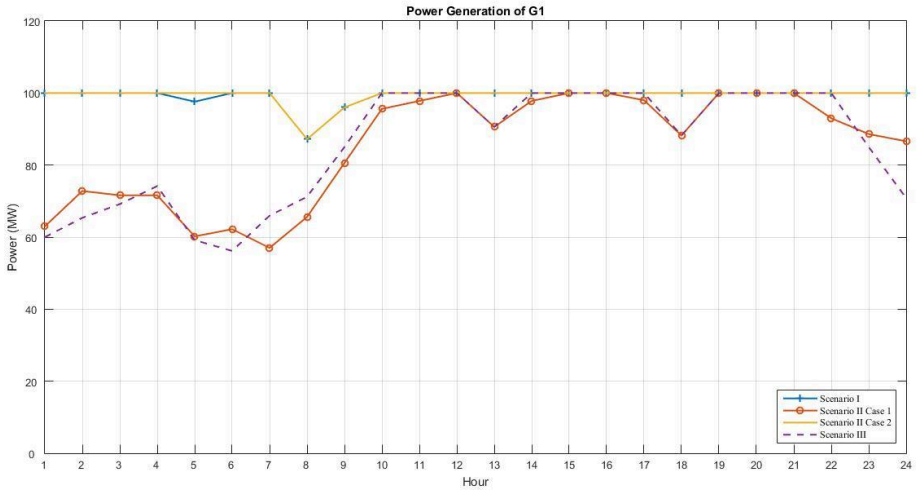

Fig. 6: Power generation profile of G1.

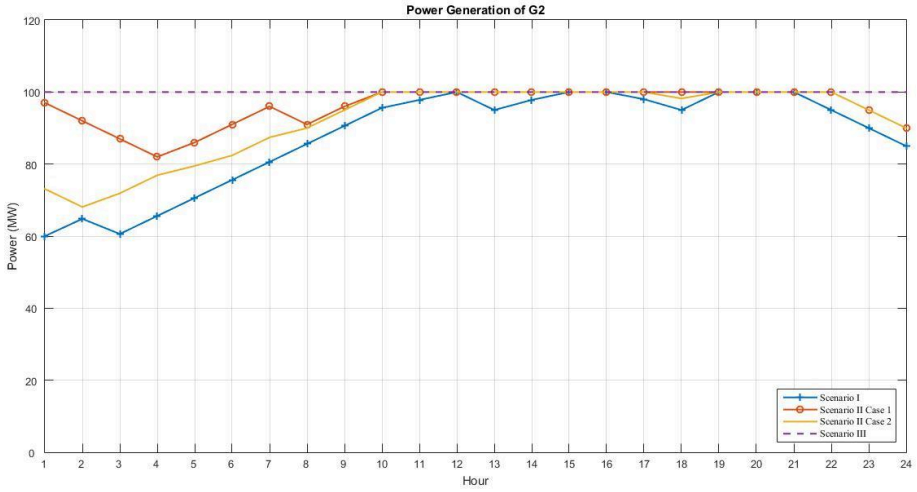

Fig. 7: Power generation profile of G2.

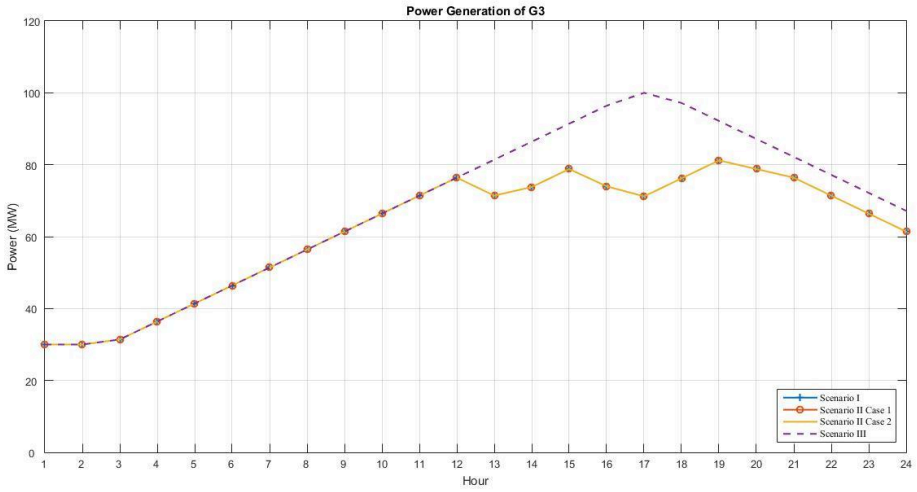

Fig. 8: Power generation profile of G3.

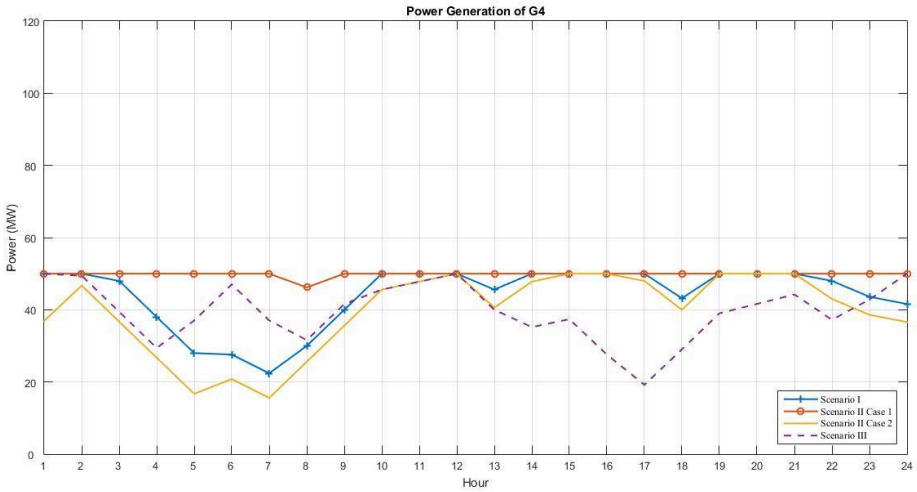

Fig. 9: Power generation profile of G4.

The TOP implementation for natural gas in all of the natural gas-fired power generators has adjusted the total gas fuel with the contract value in units G1 and G4. The power generated by gas-fired generators is adjusted to the agreed gas fuel, and the remaining generation power is borne by coal generators. Fulfillment of power by coal generators at the same capacity is supplied by generators with cheaper costs, G2 with a percentage of 34.2%. This percentage is higher than in Scenario 2 because the gas supply in Scenario 3 is less than in Scenario 2. Thus, the power generated by coal-fired generators becomes higher. Scenario 3 concludes that the TOP agreements for G1 and G4 are very impactful to the optimal operating costs. The gas production cost is increased to $279,956.88, and the electricity production is increased to $791,833.04. Thus, the optimal operating costs in Scenario 3 are higher than Scenario I by 7.67% of 791,833.04 as detailed in Table 11.

Table 11: Operating costs in Scenario 3.

Gas Supply (kcf)		Gas Production Cost ($)	Generation Cost ($)	Total Operating Cost ($)
Node 1	**Node 3**			
300	150	279,956.88	511,876.16	791,833.04

5. Conclusion

The optimal operation of IENGS by using MILP considering the TOP agreement is successfully demonstrated. This method is implemented on the integrated 6-bus electricity and 6-node natural gas systems. The optimal operation using MILP conducts optimal solutions by fulfilling the load demand and satisfying the capacity and ramp rate of generators, the capacity of transmission line, gas source, gas pipeline, and gas pressure. The simulation is focused on the optimal operating cost increase when the TOP agreement is subjected to the generation units. The TOP implementation is divided into partial and full implementation.

The detailed comparisons for optimal operating costs in all scenarios are presented in Table 12. In Scenario 1, the optimal operation was carried out without considering the TOP gas agreement, the operating costs were worth $735,405.37. In Scenario 2, the simulation was conducted in two cases. The cases are simulated based on the TOP agreement for one of the generators. In Case 1, the TOP agreement for G1 by 300 kcf increased by 3,39% of 760.320,57. While in Case 2, the TOP agreement for G4 by 150 kcf increased by 1,77% of 748.399,30. In Scenario 3, the simulation is performed with TOP agreement in all generators. The optimal operating costs are increased by 7,67% of 791.833,04.

Table 12: Comparison of operating costs in all scenarios.

Scenarios	Optimal Operating Cost ($)	Cost Increase (%)
Scenario 1	735.405,37	-
Scenario 2 Case 1	760.320,57	3,39
Scenario 2 Case 2	748.399,30	1,77
Scenario 3	791.833,04	7,67

With the success of this research, the method should be developed in the future. For example, MILP should be compared with other algorithms for in-depth performance benchmarking, such as comparing it with the learning-based algorithm that involves more advanced computation. Then, the variation of the TOP agreement scenarios for both coal-fired and natural gas-fired generators can be added for a more complex investigation. In this paper, the MILP is superior in the simulation environment, thus it can be considered for conducting future research on experimental environments, involving real-world power system parameters.

CRediT Authorship Contribution Statement

Ervina Nooraini: Writing – Original Draft, Methodology, Conceptualization, Formal analysis. **Mohamad A. Prakasa:** Writing – Original Draft, Investigation. **Muhammad R. Djalal:** Validation, Software. **Rony S. Wibowo:** Data Curation, Writing – Review & Editing. **Imam Robandi:** Writing – Review & Editing, Funding Acquisition.

Declaration of Competing Interest

The authors declare that they have no known competing financial interests or personal relationships that could have appeared to influence the work reported in this paper.

Acknowledgments

This research is sponsored by the Directorate of Research and Community Service (Direktorat Riset, Teknologi, dan Pengabdian kepada Masyarakat – DRPM), Institut Teknologi Sepuluh Nopember, under the National Grants from Ministry of Higher Education, Science, and Technology (Kementerian Pendidikan Tinggi, Sains, dan Teknologi – Kemdiktisaintek) of the Republic of Indonesia.

The researchers would to say gratitude to the members of the Power System Operation and Control (PSOC) Research Group, Power System Simulation Laboratory (PSSL), Department of Electrical Engineering, ITS, which provides material and moral assistance to researchers in conducting this work.

Data Availability

The data used for this research are available upon request to the corresponding author for those seeking to continue or replicate similar research to support further developments.

Declaration of Generative AI and AI-assisted Technologies in The Writing Process

The authors used generative AI to improve the writing clarity of this paper. They reviewed and edited the AI-assisted content and take full responsibility for the final publication.

References

[1] S. Vögele, P. Kunz, D. Rübbelke, and T. Stahlke, "Transformation pathways of phasing out coal-fired power plants in Germany," *Energy, Sustainability and Society*, vol. 8, no. 1, Aug. 2018, doi: 10.1186/s13705-018-0166-z.

[2] F. Song, H. Mehedi, C. Liang, J. Meng, Z. Chen, and F. Shi, "Review of transition paths for coal-fired power plants," *Global Energy Interconnection*, vol. 4, no. 4, pp. 354–370, Aug. 2021, doi: 10.1016/j.gloei.2021.09.007.

[3] M. A. Azni, R. Md Khalid, U. A. Hasran, and S. K. Kamarudin, "Review of the Effects of Fossil Fuels and the Need for a Hydrogen Fuel Cell Policy in Malaysia," *Sustainability*, vol. 15, no. 5, p. 4033, Feb. 2023, doi: 10.3390/su15054033.

[4] I. EA, "World Energy Outlook 2019." Paris, 2019.

[5] M. Almas Prakasa, I. Robandi, R. Nishimura, and M. Ruswandi Djalal, "A New Scheme of Harris Hawk Optimizer With Memory Saving Strategy (HHO-MSS) for Controlling Parameters of Power System Stabilizer and Virtual Inertia in Renewable Microgrid Power System," *IEEE Access*, vol. 12, pp. 73849–73878, 2024, doi: 10.1109/access.2024.3385089.

[6] M. Prakasa, I. Robandi, R. Nishimura, and M. Djalal, "A Hybrid Controlling Parameters of Power System Stabilizer and Virtual Inertia Using Harris Hawk Optimizer in Interconnected Renewable Power Systems," *IEEE Access*, p. 1, 2024, doi: 10.1109/ACCESS.2024.3405994.

[7] M. A. Prakasa, I. Robandi, A. Borghetti, M. R. Djalal, and W. Himawari, "Coordinated Design of Power System Stabilizer and Virtual Inertia Control Using Modified Harris Hawk Optimization for Improving Power System Stability," *IEEE Access*, vol. 13, pp. 2581–2603, 2025, doi: 10.1109/access.2024.3522291.

[8] M. Hafner and G. Luciani, *The Palgrave Handbook of International Energy Economics*. Springer International Publishing, 2022. doi: 10.1007/978-3-030-86884-0.

[9] W. Wei and J. Wang, *Modeling and Optimization of Interdependent Energy Infrastructures*. Springer International Publishing, 2020. doi: 10.1007/978-3-030-25958-7.

[10] International Energy Agency (IEA), "Natural Gas-Fired Electricity," 2022. [Online]. Available: https://www.iea.org/reports/natural-gas-fired-electricity

[11] Y. Zhou and C. He, "A Review on Reliability of Integrated Electricity-Gas System," *Energies*, vol. 15, no. 18, p. 6815, Sep. 2022, doi: 10.3390/en15186815.

[12] M. Khatibi, A. Rabiee, and A. Bagheri, "Integrated Electricity and Gas Systems Planning: New Opportunities, and a Detailed Assessment of Relevant Issues," *Sustainability*, vol. 15, no. 8, p. 6602, Apr. 2023, doi: 10.3390/su15086602.

[13] Y. Xu, F. Zhao, L. L. Lai, and Y. Wang, "Integrated Electricity and Natural Gas System for Day-Ahead Scheduling," in *2019 IEEE International Conference on Systems, Man and Cybernetics (SMC)*, IEEE, Oct. 2019, pp. 2242–2247. doi: 10.1109/smc.2019.8914374.

[14] Y. Zhang, Y. Hu, J. Ma, and Z. Bie, "A Mixed-Integer Linear Programming Approach to Security-Constrained Co-Optimization Expansion Planning of Natural Gas and Electricity Transmission Systems," *IEEE Transactions on Power Systems*, vol. 33, no. 6, pp. 6368–6378, Nov. 2018, doi: 10.1109/tpwrs.2018.2832192.

[15] P. Kumar, T. Mishra, and R. Banerjee, "Impact of India's power purchase agreements on electricity sector decarbonization," *Journal of Cleaner Production*, vol. 373, p. 133637, Nov. 2022, doi: 10.1016/j.jclepro.2022.133637.

[16] Asian Development Bank, "Technical Assistance Consultant's Report: Republic of Indonesia Sustainable and Inclusive Energy Program," Jan. 2018. [Online]. Available: https://www.adb.org/sites/default/files/project-documents/48323/48323-001-tacr-en_3.pdf

[17] A. Bouras, "Using goal linear programming to manage natural gas take-or-pay contract clauses in electricity generation," *Journal of Natural Gas Science and Engineering*, vol. 35, pp. 1228–1238, Sep. 2016, doi: 10.1016/j.jngse.2016.09.024.

[18] R. S. Wibowo, N. L. Nada, S. Anam, A. Soeprijanto, and O. Penangsang, "Dynamic optimal power flow with geothermal power plant under take or pay energy contract," in *2015 International Seminar on Intelligent Technology and Its Applications (ISITIA)*, IEEE, May 2015, pp. 187–192. doi: 10.1109/isitia.2015.7219977.

[19] S. Gill, I. Kockar, and G. W. Ault, "Dynamic Optimal Power Flow for Active Distribution Networks," *IEEE Transactions on Power Systems*, vol. 29, no. 1, pp. 121–131, Jan. 2014, doi: 10.1109/tpwrs.2013.2279263.

[20] M. A. Prakasa and I. Robandi, "Optimal Tuning for Power System Stabilizer using Arithmetic Optimizer Algorithm in Interconnected Two-Area Power System," in *2023 International Seminar on Intelligent Technology and Its Applications (ISITIA)*, IEEE, Jul. 2023, pp. 798–803. doi: 10.1109/isitia59021.2023.10221034.

[21] M. A. Prakasa and I. Robandi, "Tuning Improvement of Power System Stabilizer using Hybrid Harris Hawk Optimization-Equilibrium Optimizer Algorithm," in *2022 6th International Conference on Information Technology, Information Systems and Electrical Engineering (ICITISEE)*, IEEE, Dec. 2022, pp. 553–558. doi: 10.1109/icitisee57756.2022.10057700.

[22] M. F. Azis, J. Habibuddin, Mutmainnah, T. Muchtar, and D. Purwanto, "Unit commitment direct current optimal power flow using mixed-integer linear programming," *IOP Conference Series: Materials Science and Engineering*, vol. 885, no. 1, p. 12007, Jul. 2020, doi: 10.1088/1757-899x/885/1/012007.

[23] W. Meng *et al.*, "Dynamic Optimal Power Flow of Active Distribution Network Based on LSOCR and Its Application Scenarios," *Electronics*, vol. 12, no. 7, p. 1530, Mar. 2023, doi: 10.3390/electronics12071530.

[24] M. Nozarian, A. H. Nikoofard, and A. Fereidunian, "Efficient <scp>MILP</scp> formulations for <scp>AC</scp> optimal power flow to reduce computational effort," *International Transactions on Electrical Energy Systems*, vol. 30, no. 8, Apr. 2020, doi: 10.1002/2050-7038.12434.

[25] M. Usman and F. Capitanescu, "Three Solution Approaches to Stochastic Multi-Period AC Optimal Power Flow in Active Distribution Systems," *IEEE Transactions on Sustainable Energy*, vol. 14, no. 1, pp. 178–192, Jan. 2023, doi: 10.1109/tste.2022.3205213.

[26] C. Li, A. J. Conejo, P. Liu, B. P. Omell, J. D. Siirola, and I. E. Grossmann, "Mixed-integer linear programming models and algorithms for generation and transmission expansion planning of power systems," *European Journal of Operational Research*, vol. 297, no. 3, pp. 1071–1082, Mar. 2022, doi: 10.1016/j.ejor.2021.06.024.

[27] I. De Mel, O. V. Klymenko, and M. Short, "Balancing accuracy and complexity in optimisation models of distributed energy systems and microgrids with optimal power flow: A review," *Sustainable Energy Technologies and Assessments*, vol. 52, p. 102066, Aug. 2022, doi: 10.1016/j.seta.2022.102066.

[28] S. Chen, Z. Wei, G. Sun, Y. Sun, H. Zang, and Y. Zhu, "Optimal Power and Gas Flow With a Limited Number of Control Actions," *IEEE Transactions on Smart Grid*, vol. 9, no. 5, pp. 5371–5380, Sep. 2018, doi: 10.1109/tsg.2017.2687621.

[29] J. Fang, Q. Zeng, X. Ai, Z. Chen, and J. Wen, "Dynamic Optimal Energy Flow in the Integrated Natural Gas and Electrical Power Systems," *IEEE Transactions on Sustainable Energy*, vol. 9, no. 1, pp. 188–198, Jan. 2018, doi: 10.1109/tste.2017.2717600.

[30] A. J. Wood, B. F. Wollenberg, and G. B. Sheblé, *Power Generation, Operation, and Control*, 3rd ed. John Wiley & Sons, 2013.

[31] Y.-Q. Bao, M. Wu, X. Zhou, and X. Tang, "Piecewise Linear Approximation of Gas Flow Function for the Optimization of Integrated Electricity and Natural Gas System," *IEEE Access*, vol. 7, pp. 91819–91826, 2019, doi: 10.1109/access.2019.2927103.

[32] H. B. Yamchi, A. Safari, and J. M. Guerrero, "A multi-objective mixed integer linear programming model for integrated electricity-gas network expansion planning considering the impact of photovoltaic generation," *Energy*, vol. 222, p. 119933, May 2021, doi: 10.1016/j.energy.2021.119933.

[33] S. N. Emenike, A. Ioannou, and G. Falcone, "An integrated mixed integer linear programming model for resilient and sustainable natural gas supply chain," *Energy Sources, Part B: Economics, Planning, and Policy*, vol. 17, no. 1, Oct. 2022, doi: 10.1080/15567249.2022.2118901.

[34] L. Yang, X. Zhao, X. Li, X. Feng, and W. Yan, "An MILP-Based Optimal Power and Gas Flow in Electricity-gas Coupled Networks," *Energy Procedia*, vol. 158, pp. 6399–6404, Feb. 2019, doi: 10.1016/j.egypro.2019.01.203.

[35] I. Saedi, S. Mhanna, and P. Mancarella, "Integrated electricity and gas system modelling with hydrogen injections and gas composition tracking," *Applied Energy*, vol. 303, p. 117598, Dec. 2021, doi: 10.1016/j.apenergy.2021.117598.

[36] M. A. Gonzalez-Salazar, T. Kirsten, and L. Prchlik, "Review of the operational flexibility and emissions of gas- and coal-fired power plants in a future with growing renewables," *Renewable and Sustainable Energy Reviews*, vol. 82, pp. 1497–1513, Feb. 2018, doi: 10.1016/j.rser.2017.05.278.

[37] R. S. Wibowo, Nursidi, I. Satriyadi H, D. Uman P, A. Soeprijanto, and O. Penangsang, "Dynamic DC optimal power flow using quadratic programming," in *2013 International Conference on Information Technology and Electrical Engineering (ICITEE)*, IEEE, Oct. 2013, pp. 360–364. doi: 10.1109/iciteed.2013.6676268.